Chapter- 5

Results and Discussion

Mechanical and tribological properties of CNTs, GO, and (CNTs/GO) hybrid coated carbon FREC

This chapter details the physical and thermal characterization of carbon fibers treated with chemical agents, along with the application of CNTs, GO, and CNT/GO hybrid coatings. Techniques such as FTIR, SEM, and TGA were employed to analyze the fibers and coatings. The study further evaluates the physical, mechanical, thermal, and tribological properties of the resulting carbon fiber-reinforced polymer composites using methods like density measurement, tensile testing, hardness testing, impact and flexural testing, ILSS testing, thermal conductivity evaluation, and tribological analysis. SEM was utilized to inspect the wear patterns on the composite surfaces, offering insights into their wear mechanisms and surface morphology. These thorough characterizations provide a deeper understanding of the composite materials' performance across different conditions, demonstrating their potential for a wide range of applications.

5.1 FTIR analysis

5.1.1 Infrared Spectroscopy of CNT

The details of FTIR analysis of chemically treated and untreated CNT are already discussed in section 4.1.1 in chapter 4.

5.1.2 Infrared Spectroscopy of Carbon Fiber

Figure 5.1 shows the FTIR analysis of untreated aramid fiber and chemically treated (functionalized) aramid fiber, which is performed in between 500 to 4000 cm^{-1} wave

number. In Figure 5.1, the peak at 1376 cm^{-1} corresponds to C-H bending vibrations, indicating the presence of methyl group [219]. Peaks observed at 1640 cm^{-1} are attributed to C=O stretching vibrations, associated with carboxyl functional groups introduced during the acid treatment [193, 194]. A broad absorption band around 3447 cm^{-1} corresponds to O–H stretching, indicating the presence of hydroxyl groups on the fiber surface [220]. Furthermore, when untreated carbon fibers were immersed in a 3 M acid mixture of sulphuric and nitric acids, the sizing agents were effectively removed. This was evident from the reduced intensity of the methylene stretching peak at 2915 cm^{-1} in treated fibers compared to untreated ones [196]. Simultaneously, the treated fibers showed enhanced peak intensities at 3447 cm^{-1} (O–H) and 1640 cm^{-1} (C=O), indicating the successful incorporation of hydroxyl and carboxyl groups. These spectral changes confirm the oxidative functionalization and increased surface activity of the carbon fibers after acid treatment [197].

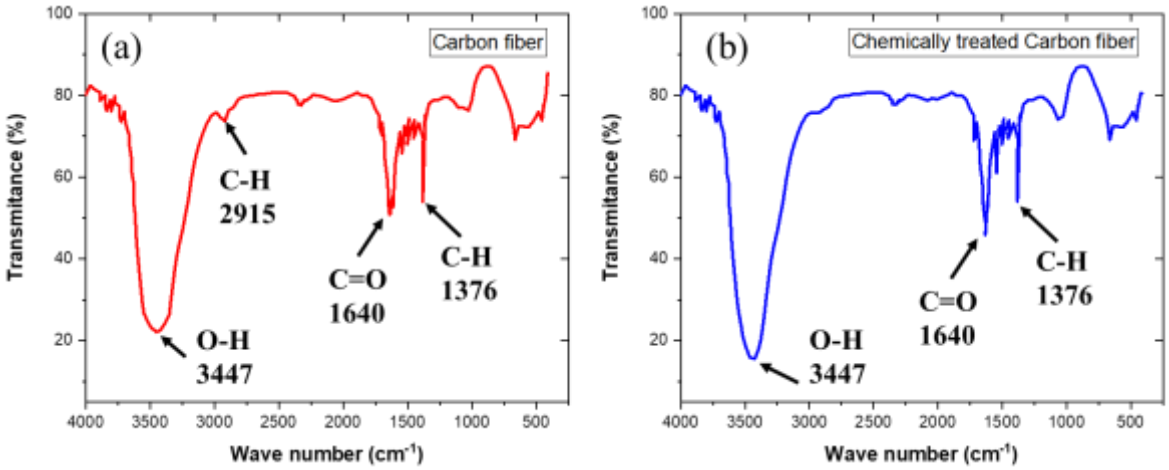

Figure 5.1 FTIR spectra of (a) Untreated Carbon fiber, (b) Chemically treated Carbon fiber

5.2 Thermogravimetric analysis of carbon fiber and Nanoparticles coated carbon fiber

Figure 5.2 illustrates the TGA curves for both the carbon fiber and the carbon fiber coated with nanoparticles. In these curves, the plateau region indicates the thermal stability

range of the fiber, while the steep section corresponds to the phase of weight loss. As seen in Figure 5.2, the thermogravimetric curves, which range in temperature from 24 °C to 800 °C, may be separated into two phases. The first stage of thermal degradation is linked to the extraction of moisture content and waxy components from the fibers, and it happens between 24 °C and 550 °C. Both uncoated and nanoparticle-coated carbon fiber lose about 1-3 percent of its weight in this temperature range [198]. Carbon fiber remains stable up to 550°C in air, beyond which rapid decomposition occurs due to oxidation of carbon fiber [140, 221]. In the temperature range of 550°C to 800°C, uncoated carbon fiber undergoes an 11.2% weight loss, while CNTs-coated, GO-coated, and CNTs/GO-coated carbon fibers experience reduced weight losses of 8.21%, 7.21%, and 6.12%, respectively. The protective barriers provided by GO and CNTs contribute to enhanced thermal stability. The total weight losses for uncoated, CNTs-coated, GO-coated, and CNTs/GO-coated carbon fibers are 13%, 11.21%, 10.21%, and 8.45%, respectively. Incorporating CNTs and GO improves heat resistance, which is attributed to their exceptional thermal properties [222]. The enhanced thermal stability is associated with the facilitation of heat dissipation by CNTs and GO, preventing the formation of localized hot spots in coated carbon fiber [223, 224].

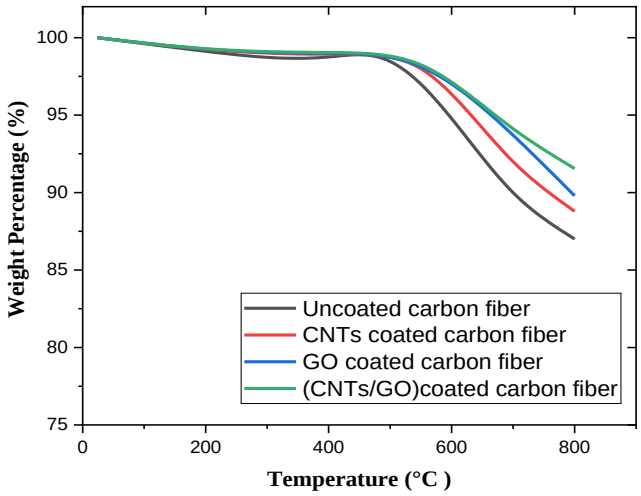

Figure 5.2 TGA curves of uncoated carbon fiber, CNT-coated aramid fiber, GO-coated carbon fiber, and (CNTs/GO) hybrid-coated carbon fiber

5.3 Scanning electron microscopy (SEM)

The surface morphologies of CF, GO-coated CF, CNTs-coated CF, and CNTs/GO hybrid-coated CF are shown in Figure 5.3. Because of the Polyacrylonitrile precursor spinning process, the surface of the non-coated CF Figure 5.3(a) has continuous ridges and grooves running down the fiber axis, giving the impression of being relatively smooth. The introduction of carbon nanomaterials alters the surface topography of CF. In Figure 5.3(b), CNTs exhibited a random orientation, wrapping around the surfaces of carbon fibers (CF) with minimal aggregation. This resulted in the formation of a rough surface characterized by numerous protrusions [66].

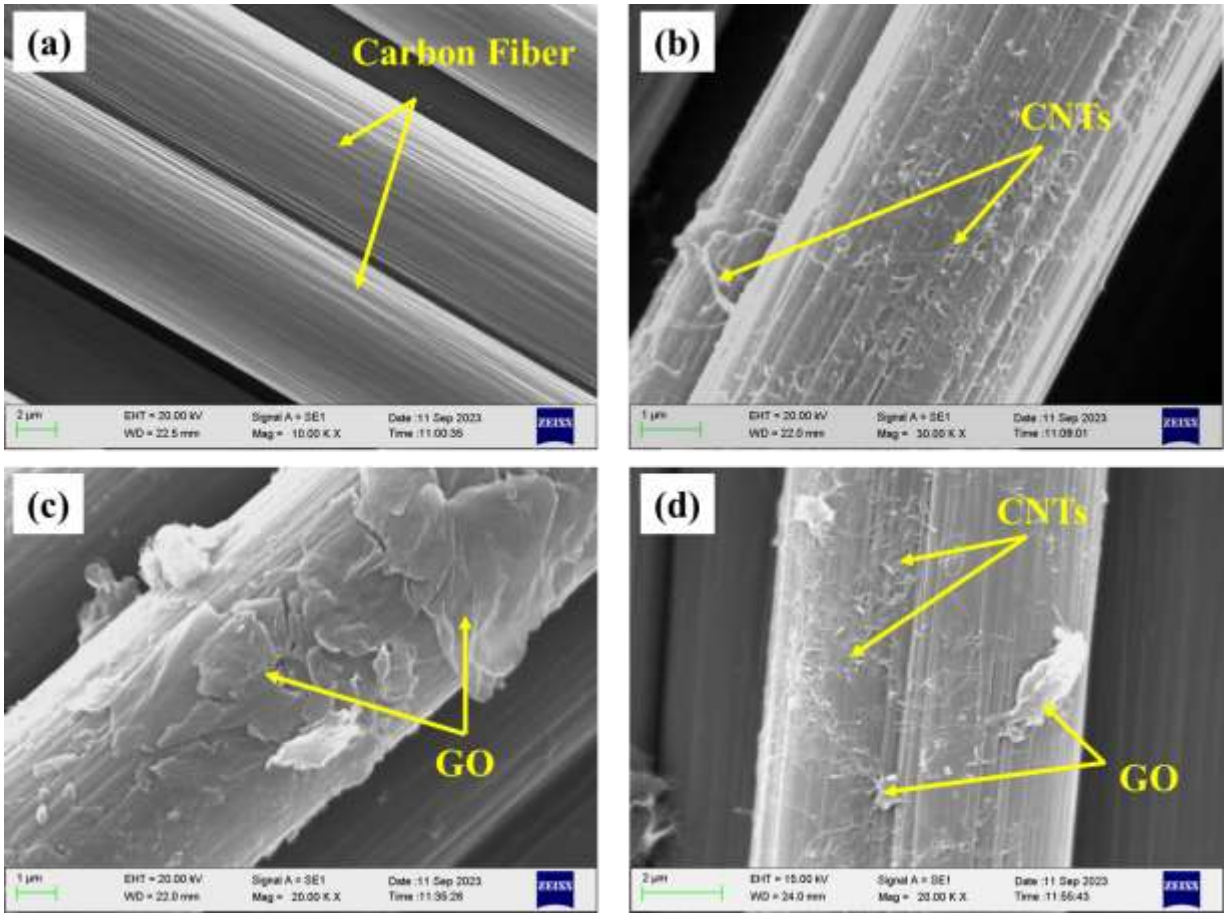

Figure 5.3 The surface morphology of carbon fiber (a) uncoated CF, (b) CNTs coated CF, (c) GO coated CF, (d) CNTs/GO hybrid coated CF

Under the same modification circumstances, GO is equally distributed over CF surfaces Figure 5.3(c). The CNTs/GO hybrid coating layer Figure 5.3(d) shows a uniform distribution on CF surfaces. The attachment of CNTs and GO to CF surfaces enhances surface contact points and interactions between CF and the epoxy matrix. This enhancement is beneficial for improving the mechanical and interfacial properties of carbon fiber-reinforced epoxy (CFRE) composites [225].

5.4 Density calculation

Table 5.1 Density calculation of CFRE, CCFRE, GCFRE, and HCFRE composites.

S. No	CFRE (mass in air) (gm)	CFRE (mass immersed in water) (gm)	Specific Gravity	Density (Kg/m^3)
1.	1.706	0.422	1.3286	1324.6142
2.	1.708	0.421	1.3256	1321.6232
S. No	CCFRE (mass in air) (gm)	CCFRE (mass immersed in water) (gm)	Specific Gravity	Density (Kg/m^3)
1.	2.260	0.503	1.2862	1282.3414
2.	2.257	0.501	1.2853	1281.4441
S. No	GCFRE(mass in air) (gm)	GCFRE (mass immersed in water) (gm)	Specific Gravity	Density (Kg/m^3)
1.	1.729	0.417	1.3178	1313.8466
2.	1.732	0.415	1.3151	1311.1547
S. No	HCFRE (mass in air) (gm)	HCFRE (mass immersed in water) (gm)	Specific Gravity	Density (Kg/m^3)
1.	1.762	0.412	1.3051	1301.1847
2.	1.759	0.409	1.3029	1298.9913

The four different polymer composites exhibited specific gravities and densities, as detailed in Table 5.1. The average density of CFRE, CCFRE, GCFRE, and HCFRE composite samples was determined to be 1323.1187 kg/m^3, 1281.89275 kg/m^3, 1312.5006 kg/m^3, and 1300.088 kg/m^3, respectively. Compared to the other four polymer composites, CCFRE exhibits the lowest density, while CFRE displays the highest density.

5.5 Microhardness test

The sample' surface was marked with ten different indentations, and measurements of the microhardness were made at each location. The hardness of the specimens was then determined by averaging the 10 values. This data was presented on a bar chart in Figure 5.4, including the standard deviation for each measurement. Figure 5.4 compares hardness values among four types of polymer composites. CFRE exhibited the lowest hardness value, measured at 20.83 HV. The increase in hardness values observed in the polymer composites can be attributed to the coating of nanoparticles on the fibers.

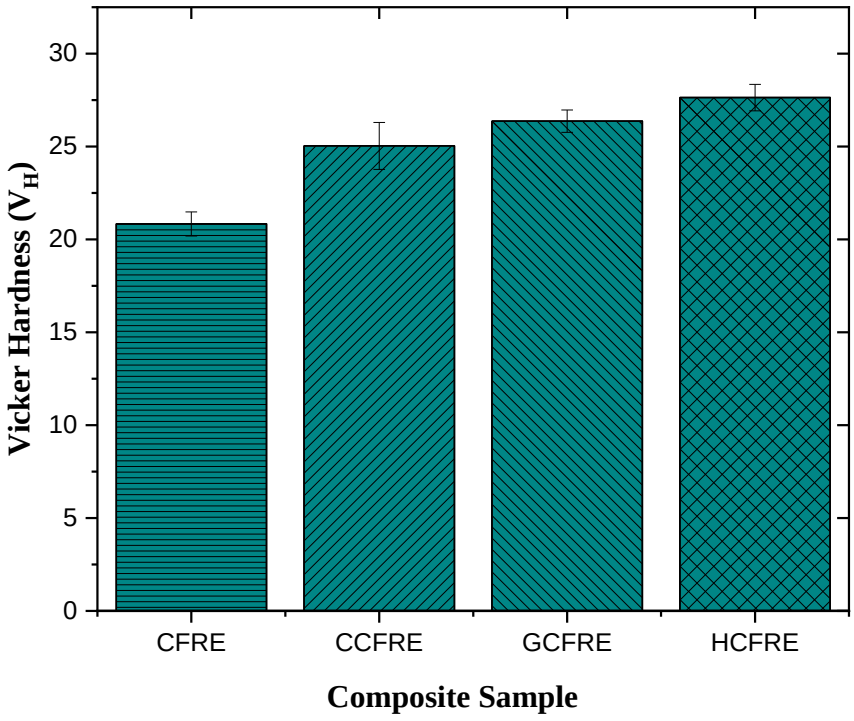

Figure 5.4 Vickers hardness value of different fiber reinforced polymer composites

This coating enhances the interfacial bonding between the matrix and fibers, which reduces the mobility of interface shear bonds and helps mitigate deformation induced by external forces, consequently enhancing the hardness of the polymer composite [66]. The hardness of HCFRE surpassed all other polymer composites, showing a remarkable 32.64% increase compared to CFRE. This notable enhancement in hardness is attributed to the synergistic and bridging effects of 1-D (CNTs) and 2-D (GO) present in the composites [226].

5.6 Tensile testing

Five specimens were subjected to tensile testing for each type of polymer composite, including CFRE, CCFRE, GCFRE, and HCFRE, to assess the impact of woven carbon fiber and nanoparticles-coated carbon fibers on the resulting composite laminates' tensile properties. The stress-strain curves for these specimens are illustrated in Figure 5.5, indicating the brittleness of the composite as evidenced by the measured strain levels. Incorporating CNTs/GO increased the brittleness while enhancing the composite's strength, which is reflected higher failure stress.

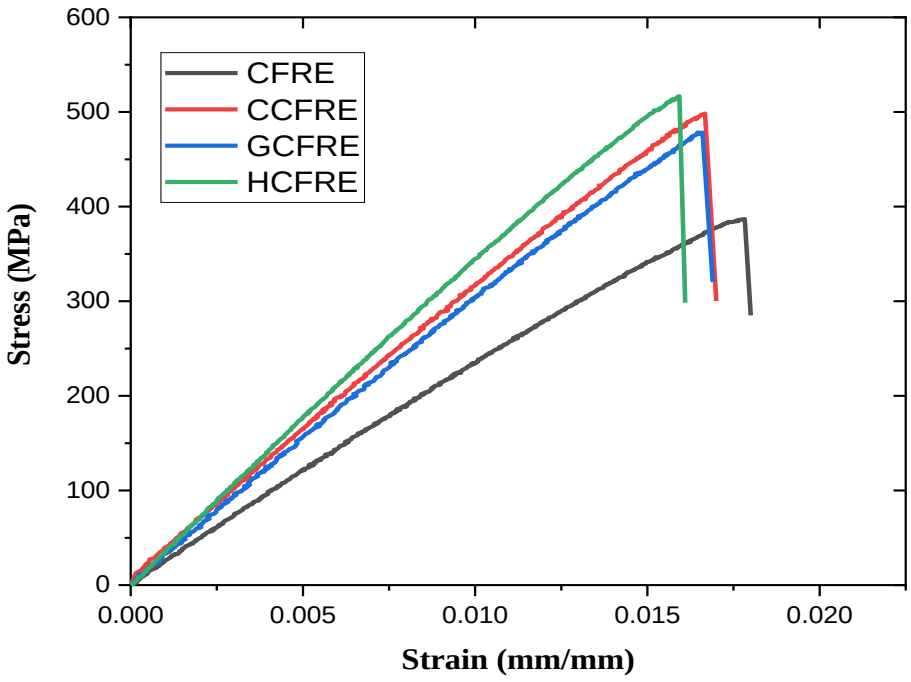

Figure 5.5 Stress-strain curves of different fiber-reinforced polymer composites.

Figures 5.6(a) and 5.6(b) show the tensile strength and tensile modulus obtained from the stress-strain curve analysis, respectively. Notably, CCFRE, GCFRE, and HCFRE exhibit superior tensile strength and modulus compared to CFRE, indicating the reinforcing effect of CNTs/GO. CCFRE significantly enhances tensile modulus and tensile strength, surpassing CFRE by 25.95%, and 27.94%, respectively. The kinked and twisted structure of CNTs, which create mechanical interlocks with the matrix, is credited with this enhancement [208], preventing polymer chain movement under load and enhancing tensile properties [210]. Similarly, GCFRE displays increased tensile modulus and strength with improvements of 22.33% and 23.22%, respectively, relative to CFRE. The reason for this improvement is the layered and wrinkled sheet structure of GO, which prevents cracks from propagating inside the polymer matrix and increases energy dissipation [143]. Moreover, CCFRE exhibits higher tensile strength and modulus compared to GCFRE, primarily due to GO tendency to aggregate owing to its larger surface area [227].

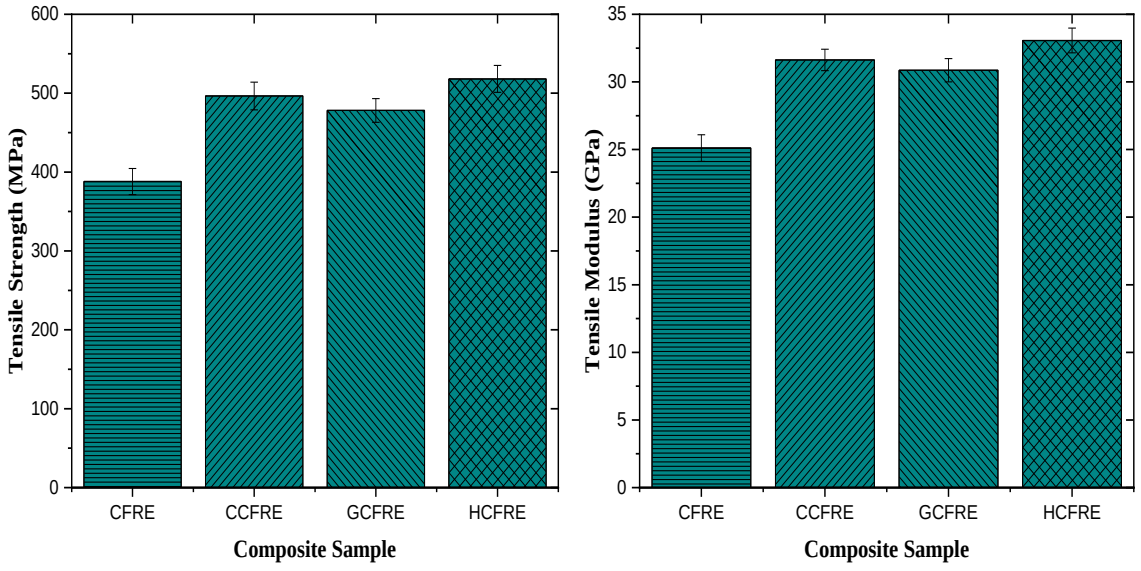

(a) (b)

Figure 5.6 Tensile strength (a) and tensile modulus (b) of fiber-reinforced polymer composites.

According to Figures 5.5 and 5.6, HCFRE demonstrates the highest tensile modulus of 33.06 GPa and tensile strength of 518.09 MPa among all four composite specimens. This represents an increase of 33.53% tensile strength and 31.66% tensile modulus as compared to CFRE. Combining one-dimensional CNTs and two-dimensional GO structures facilitates the formation of a rod-sheet network, synergistically enhancing the composite's tensile properties [143]. The tensile strength of polymer composite laminates is bolstered by factors such as the durability of the matrix material, the level of interfacial adhesion, and the effective dispersion of particles or fibers within the matrix [206]. CF smooth surface usually shows poor interfacial adhesion between the fiber strand and matrix. Nevertheless, better interfacial bonding between the fiber and epoxy is produced by the deposition of CNTs or GO onto CF, allowing for more efficient stress transmission from the epoxy to the fiber [207]. The remarkable mechanical properties of CNTs and GO are also instrumental in enhancing the tensile properties of the epoxy composite [209].

5.7 Flexural testing

The flexural stiffness and strength play a critical role in ensuring the structural integrity of composites, particularly in scenarios involving high loads and sliding velocities, where preventing deformation and bending failure is paramount. To address this concern, the flexural characteristics of CFRE composites, both with and without coatings of CNTs, GO, and a hybrid of GO/CNTs, were investigated using a three-point bending test. The flexural strength and flexural modulus for the fiber-reinforced polymer composites are shown in Figure 5.7 (a) and (b), respectively.

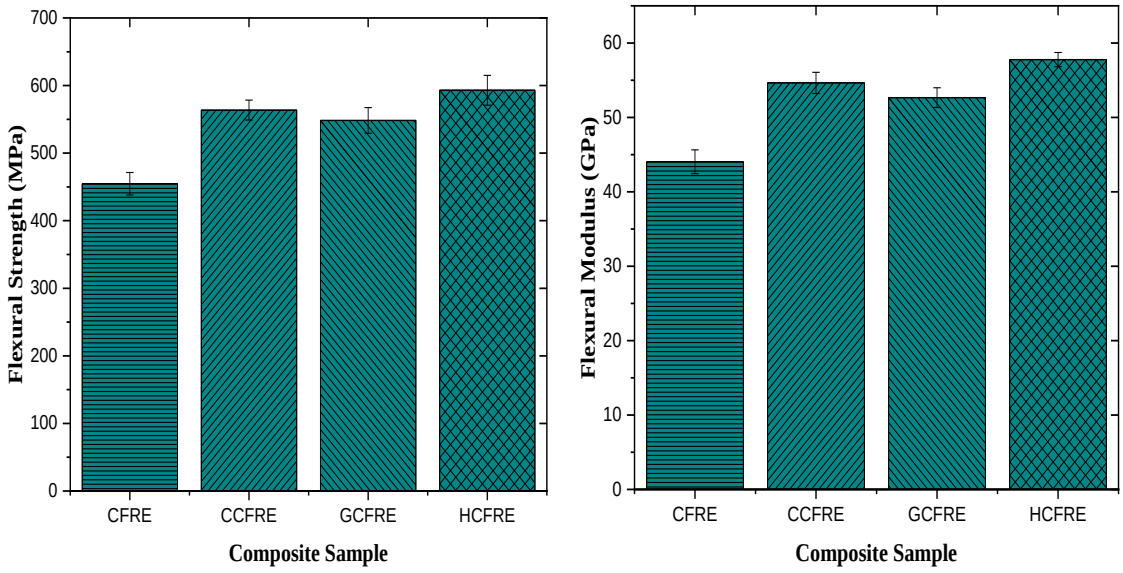

(a) **(b)**

Figure 5.7 Flexural strength (a) and flexural modulus (b) of fiber-reinforced polymer composites.

As illustrated in Figure 5.7, the flexural strength and flexural modulus of CFRE without any coating are recorded at 454.78 MPa and 44.04 GPa, respectively. The flexural strength of CCFRE and GCFRE composites was measured at 563.7 MPa and 548.27 MPa, respectively, showing an increase of 23.95% and 20.55% compared to the CFRE composite. Additionally, the flexural modulus of CCFRE and GCFRE composites was observed as 54.64 GPa and 52.66 GPa, respectively, demonstrating an increase of 24.06% and 19.57% compared to the CFRE composite. The mechanical properties of the composite were improved by applying a coating consisting of CNTs or GO onto the carbon fiber. This improvement can be attributed to the significant aspect ratio, large surface area, superior stiffness, and flexural modulus of these nanoparticles [228]. From Figure 5.7, HCFRE demonstrates the highest flexural modulus of 57.77 GPa and flexural strength of 593.07 MPa among all four composite specimens. This represents an increase of 30.40% flexural strength and 31.17% flexural modulus compared to CFRE, demonstrating the synergetic effect of GO and CNTs in the hybrid coating [225].

5.8 Short Beam Shear (SBS) test

This test is crucial for assessing the ILSS of fiber composites due to their layered structures, which are highly responsive to shear loading. The outcomes of the (SBS) test are depicted in Figure 5.8, illustrating the effects of coated and uncoated carbon fiber-reinforced epoxy composites. The ILSS value of the CFRE composite is 21.66 MPa. The results indicate that the ILSS of CCFRE, GCFRE, and HCFRE hybrid-coated CFRP composites is approximately 29.45%, 27.7%, and 38.73% higher, respectively, compared to CFRE composites. The outcome suggests that incorporating GO, CNTs, and a CNTs/GO hybrid into the interphase of fiber-reinforced polymer composites notably enhances their interfacial properties. Among these coatings, the CNTs/GO hybrid coating is the most efficient in enhancing interlaminar shear strength, indicating a clear synergistic effect [225, 229].

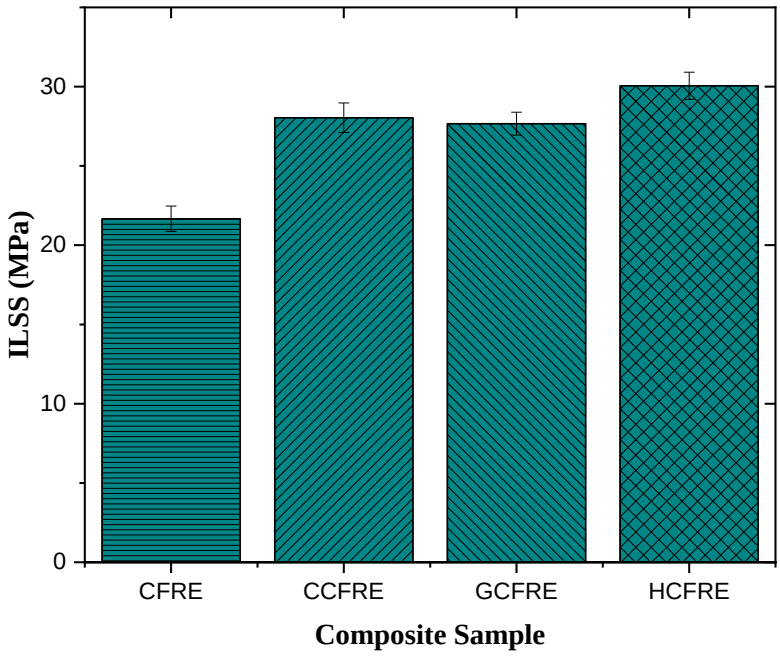

Figure 5.8 ILSS of fiber-reinforced epoxy composites.

The presence of CNTs/GO on the carbon fiber surface enhances the toughness of the epoxy resin near the interface by inducing plastic deformation and extraction of the epoxy resin.

This phenomenon aids in improving interfacial stress transfer and strain resistance, thereby allowing for greater energy dissipation during the shear failure process of the interface. Consequently, this effectively enhances the ILSS of fiber-reinforced polymer composites coated with GO/CNTs hybrids [207].

5.9 Impact test

The fracture toughness resulting from impact is an important aspect in analyzing the failure of composite materials. When subjected to impacts, composites absorb some energy involved in various failure mechanisms such as interlayer failure, delamination, matrix cracking, and fiber breakage [230]. Figure 5.9 illustrates the impact energy performance of carbon fiber-reinforced epoxy composites with and without coatings. It is evident that applying coatings of CNTs, GO, and CNTs/GO hybrid nanoparticles onto the carbon fibers enhances the composites' impact strength. The impact energy of the CFRE composite measures 9.13 J/cm^2. The findings demonstrate a 26.94% increase in impact energy for CCFRE and a 24.64% increase for GCFRE compared to the CFRE composite. Incorporating CNTs or GO improves the bonding between the filler, matrix, and fiber enhancing interfacial adhesion [99].

This enhancement contributes to greater impact energy absorption and diminishes interlaminar fracture tendencies within the composites [231]. HCFRE achieves the highest impact energy value of 12.43 J/cm^2, marking a 36.36% increment compared to the CFRE composite, owing to the synergistic effects of CNTs/GO. The interlocking mechanism between coated fibers and epoxy significantly enhances the properties of the carbon/epoxy composites [232].

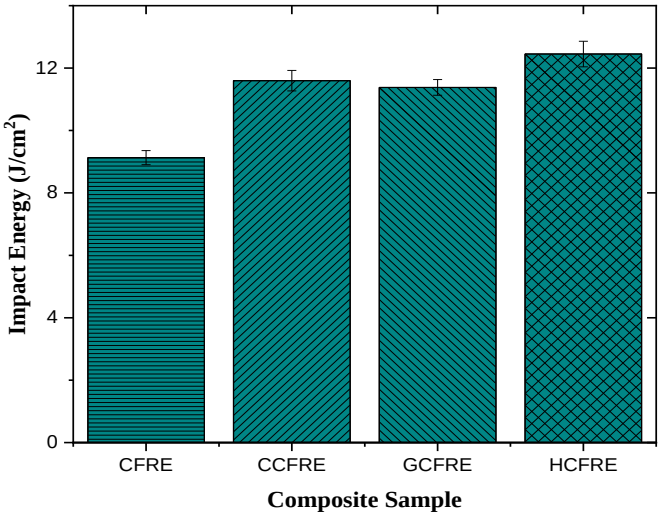

Figure 5.9 Impact energy of fiber-reinforced epoxy composites.

5.10 Thermal conductivity test

Figure 5.10 shows the thermal conductivity of the CFRE, CCFRE, GCFRE, and HCFRE composites. Composites containing CNTs (CCFRE) and GO (GCFRE) exhibit thermal conductivities of 0.355 W/mK and 0.342 W/mK, respectively, representing a 36.18% and 30.85% increase compared to the CFRE composite. The high specific surface area and superior heat conductivity of GO and CNTs are responsible for this improvement [233, 234].

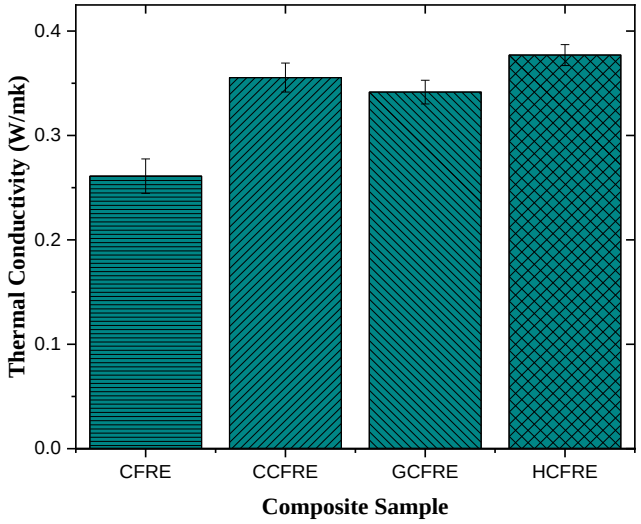

Figure 5.10 Thermal conductivity of fiber-reinforced epoxy composites.

The HCFRE composite demonstrates the highest thermal conductivity of 0.377 W/mK among the composites due to the synergistic effect of the 1-D rod-like structure of CNTs and the 2-D sheet structure of GO, which creates thermal conductivity bridges, thereby enhancing heat flow [235]. Consequently, introducing CNTs and GO simultaneously into composites significantly improves their thermal conductivity, which in turn improves the tribological performance of the fiber-reinforced epoxy composites [143].

5.11 Tribological testing

5.11.1 Effect of GO, CNTs, and hybrid (GO/CNTs) coating on the tribological properties of CFRE composites.

Figure 5.11 illustrates the evolution of the friction coefficient for CFRE, CCFRE, GCFRE, and HCFRE composites during a 9600-cycle test conducted at room temperature. The test is carried at a normal load of 40 N, a to and fro sliding frequency of 8 Hz, and a stroke length of 1.5 mm. Initially, composites experienced an increased friction coefficient attributed to matrix plasticization, leading to adhesion between the matrix and the steel ball's surface, along with surface delamination of the composite material [212]. However, carbon fiber fragments emerged after several cycles, acting as third-body particles. These fragments circulated between interacting surfaces, forming a layer of friction that substantially reduced the coefficient of friction before reaching a stable state over a period. It was also observed from Figure 5.11 that the COF of CCFRE, GCFRE, and HCFRE was lower than that of CFRE composite because of the self-lubricating properties, high load-bearing capacity, and high wear resistance of GO and CNTs [236]. From Figure 5.12 it is clearly observed that the CCFRE, GCFRE, and HCFRE composites experience reduced weight loss and specific wear rates compared to the CFRE composite. This difference can be ascribed to incorporating CNTs, GO, or both, which were applied as a coating on the

carbon fiber within the polymer composite. The composite's resistance to wear was eventually improved by this coating's improvement of interfacial adhesion. The CFRE composite has a specific wear rate of 23.62(*10^{-4} mm^3/Nm).

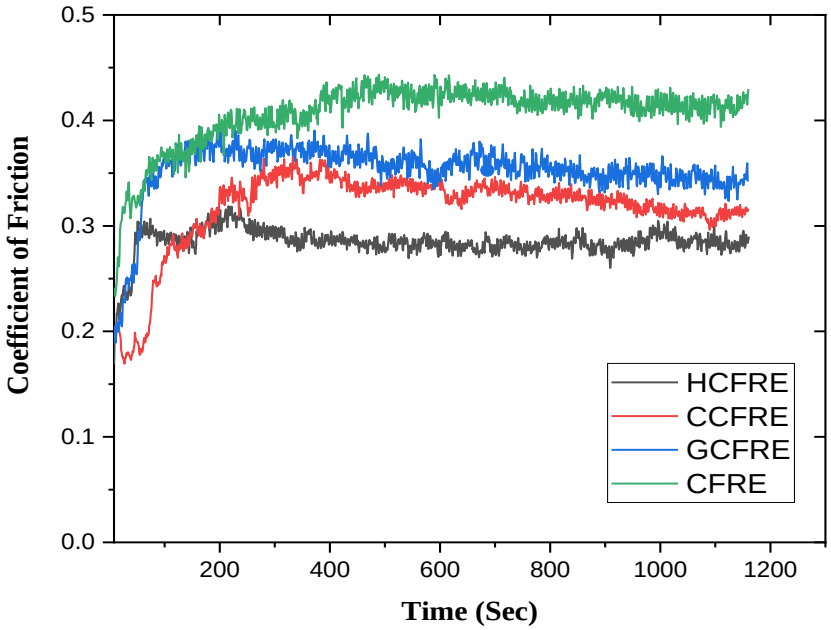

Figure 5.11 Coefficient of friction vs time for CFRE, CCFRE, GCFRE, and composite at (40 N, 8Hz).

The study found a 27.26% decrease in specific wear rate for CCFRE compared to CFRE, suggesting that CNTs at the fiber-matrix interface promote the formation of a durable tribo-film, reducing wear [160]. Additionally, CNTs act as micro-bearings, converting sliding friction to rolling friction, further reducing wear and COF [237, 238]. Similarly, GCFRE showed a significant 23.45% decrease in specific wear rate compared to CFRE, attributed to solid film formation by GO due to weak van der Waals forces between GO sheets [183]. The improved mechanical interlocking induced from the wrinkled rough surface of GO enhances interfacial adhesion between matrix and fiber, indicating that adding GO to Carbon fiber/Epoxy composites improves wear resistance by reducing abrasive wear [239, 240]. HCFRE observed the minimum specific wear rate, which was 42.84% less than the CFRE composite because of the synergetic effect of

CNTs/GO hybrid coated carbon fiber reinforced polymer composite. Flexible carbon nanotubes (CNTs) can penetrate between GO, preventing them from aggregating face-to-face. Van der Waals forces cause GO to infiltrate between CNTs and create complementary structures that interact to prevent restacking [241]. This suggests that the hybrid coating of GO and CNTs can easily form a 3D structure of hybrid carbon nanomaterials, leading to increased surface area. This enhanced surface area improves contact and interlocking at the interface between the matrix and carbon fibers, ultimately enhancing interfacial adhesion. Moreover, incorporating GO and CNTs will enhance wear resistance by uniformly dispersing stress throughout the matrix [242]. The findings showed great enhancement in friction and wear properties due to the surface modification of carbon fiber with CNTs and GO [243].

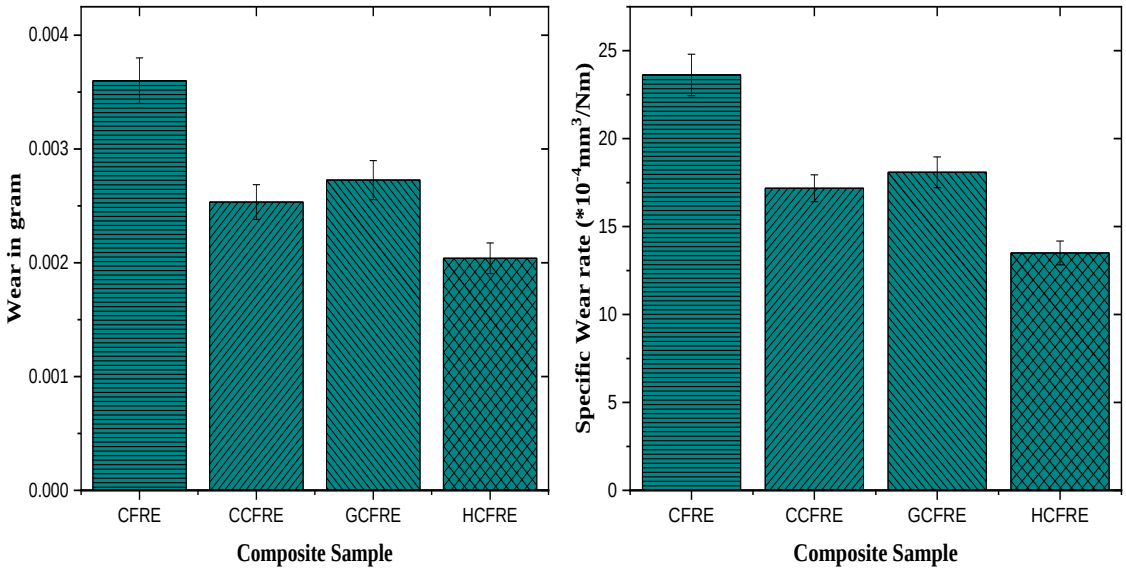

(a) **(b)**

Figure 5.12 Variation of (a) wear in gram and (b) specific wear rate of CFRE, CCFRE, GCFRE, and HCFRE composite at (40 N, 8Hz).

5.11.2 Effect of load on friction coefficient of fiber-reinforced polymer composite.

The COF values for CFRE, CCFRE, GCFRE, and HCFRE composites are shown in Figure 5.13 with varied normal loads (30 N, 40 N, 50 N, and 60 N) at a constant frequency of 8 Hz. The findings suggest that as the applied normal load increases, the coefficient of friction (COF) also increases across different polymer composite samples. This phenomenon can be attributed to the increased contact pressure between the steel ball and the specimen under higher loads, potentially elevating the interface temperature and reinforcing the adhesive component of friction [217]. Furthermore, asperities penetrate significantly at higher loads, increasing the frictional force and contributing significantly to the abrasion component of the friction coefficient, thus, the increase in the COF at higher normal loads can likely be attributed to these factors. At a normal load of 30 N, the HCFRE composite demonstrates the lowest COF value of 0.234, while the CFRE composite exhibits the highest COF value of 0.41 at a normal load of 60 N.

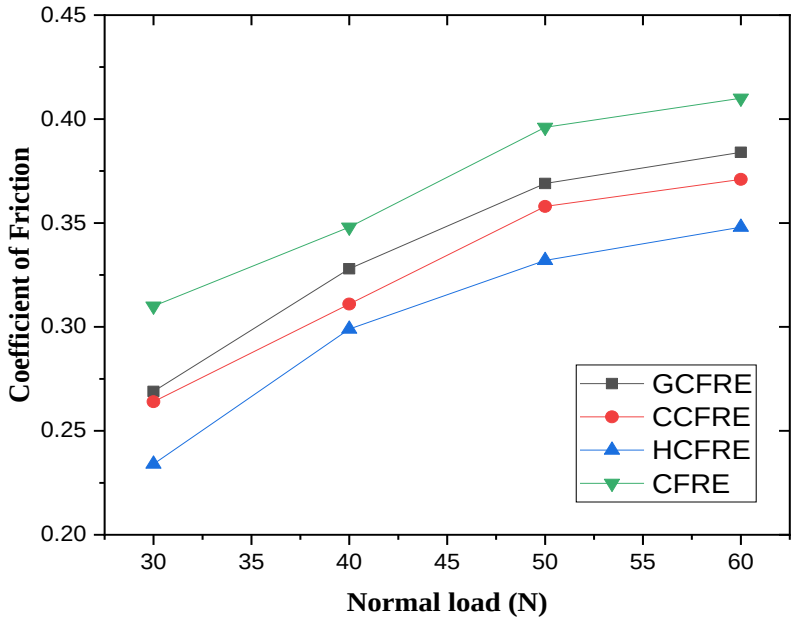

Figure 5.13 Variation of Friction coefficient with load at a constant frequency of 8 Hz.

5.11.3 Effect of sliding frequency on friction coefficient of fiber-reinforced polymer composite.

The COF values for CFRE, CCFRE, GCFRE, and HCFRE polymer composites are shown in Figure 5.14 at different frequencies (6, 8, 10, and 12 Hz) under a constant normal load of 40 N. For all four polymer composites, it is observed that COF decreasing with increasing sliding frequency. This decreasing is explained by the higher reciprocating sliding frequency, which causes the polymer matrix to soften and plastic deformation [244]. By lowering adhesion force and plowing action, carbon fibers improve the polymer composite's frictional properties. A similar tendency of COF decreasing with sliding frequency was also observed by Guo et al. [218] who attributed this to surface softening brought on by frictional heating. With a friction coefficient value of 0.277 at 12 Hz, the HCFRE composite had the lowest value, while at 6 Hz, the CFRE composite had the highest value, 0.354.

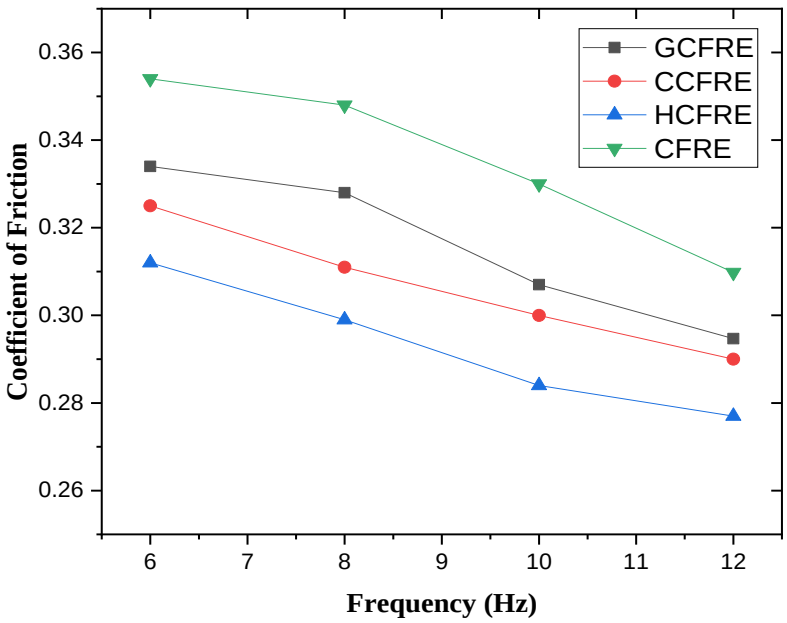

Figure 5.14 Variation of Friction coefficient with frequency at a constant load of 40 N.

5.12 SEM analysis of worn surface

Figure 5.15 displays the SEM of the worn surfaces of the CFRE, CCFRE, GCFRE, and HCFRE polymer composites under the identical conditions (40 N, 8 Hz). Figure 5.15 (a) shows that maximum breakage of matrix and fiber was found in the CFRE composite because of the poor interfacial adhesion and mechanical interlocking between the fibers and matrix [245]. In the CFRE composites, the surface displayed extensive matrix breakdown, with most fibers in the top layer disconnected. The worn surfaces from sliding exhibited notable fiber breakage, debonding, and removal, along with instances of fiber pull-out due to inadequate fiber-matrix adhesion. In CNTs, GO, and hybrid coated fiber polymer composite samples, as shown in Figure 5.15 (b-d), have minimal empty fiber slots, fiber damage, and matrix removal due to adhesion were observed, indicating enhanced bond strength between fibers and the matrix, thus hindering fiber pull-out [246]. Additionally, residual stresses generated during curing can lead to stress concentration and separation between the fiber and matrix. Nanoparticles coated on fiber alleviate these stresses through mechanical locking, enhancing interfacial strength between fiber and matrix, increasing the stress required for fiber breakage and pull-out [247].

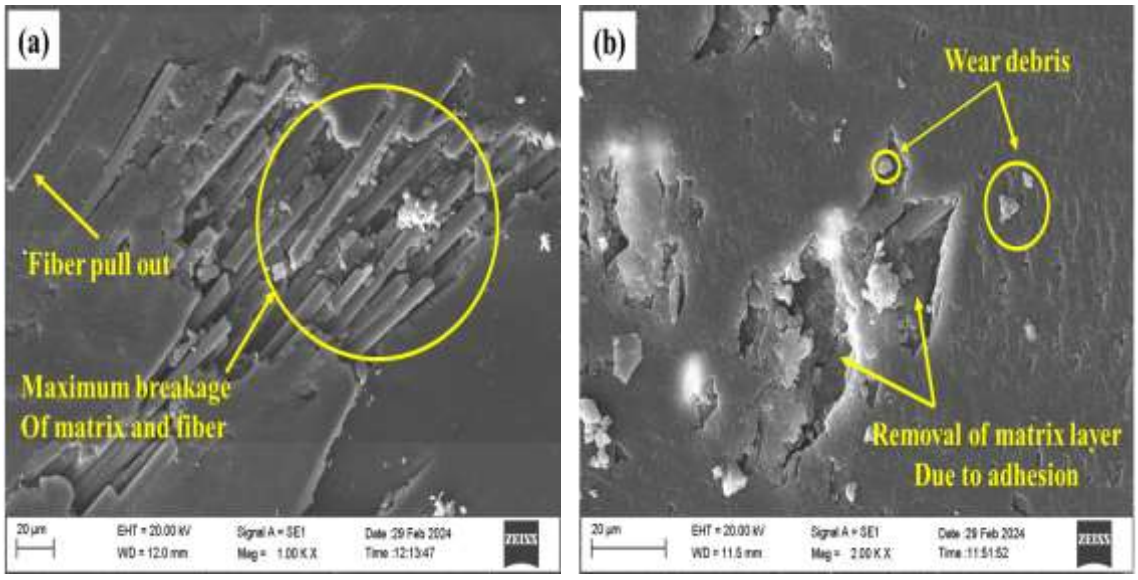

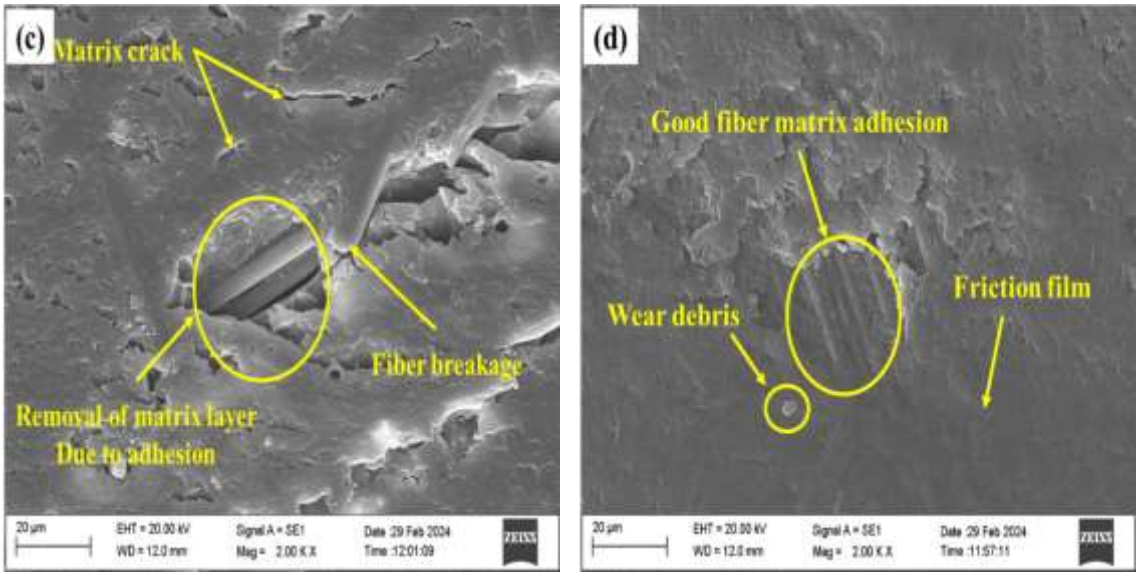

Figure 5.15 SEM images of worn surfaces of (a) CFRE, (b) CCFRE, (c) GCFRE, and (d) HCFRE under the same condition (40 N, 8Hz).

From Figure 5.15 (d), it was clear that the HCFRE composite exhibited excellent fiber-matrix adhesion and minimal removal of the matrix layer, attributed to the combined effect of CNTs and GO. This synergy likely arises from the high thermal conductivity of the composite, which aids in dissipating frictional heat from the interface region, along with the lubricating effect of CNTs and GO [248]. Additionally, in the HCFRE composite, wear debris containing CNTs and GO, which adhered to the counter face, forming a friction film layer at the interface. This layer significantly reduced the coefficient of friction and specific wear rate.

5.13 Summary

The findings can be summarized as follows:

- CNTs, GO, and hybrid (CNTs/GO) coatings enhance interfacial bonding by increasing surface roughness, improving matrix adhesion in epoxy composites.
- TGA analysis confirms enhanced thermal stability due to CNTs and GO protective barriers.

- A three-dimensional CNT/GO network synergistically enhances mechanical and interfacial properties, leading to the highest ILSS, flexural strength, tensile strength, and hardness in coated composites.
- HCFRE composite achieves 36.36% higher fracture toughness, 57.68% improved flexural modulus, and the highest thermal conductivity of 0.377 W/mK.
- CNTs/GO hybrid coating reduces specific wear rate by 42.84%, enhancing durability, while COF decreases with increasing sliding frequency however, increases with increasing load.
- SEM analysis reveals enhanced fiber-matrix adhesion and minimized surface damage in nanoparticle-coated fiber-reinforced polymer composites, establishing them as high-performance materials for advanced engineering applications.